Advances in Environmental Technology 1 (2018) 1-12

Advances in Environmental Technology

journal homepage: http://aet.irost.ir

Thermal and chemical modification of bentonite for adsorption of an anionic dye

Elahe Rostami, Reza Norouzbeigi*, Ahamd Rahbar Kelishami

School of Chemical, Petroleum and Gas Engineering, Iran University of Science and Technology (IUST), Tehran, Iran

ARTICLE INFO

Article history:
Received 21 December 2016
Received in revised form
13 June 2018
Accepted 20 June 2018

Keywords:
Adsorption
Bentonite
Congo red
Langmuir
Thermal and chemical modification

ABSTRACT

Raw bentonite (RB), a known low-cost versatile clay was used as an adsorbent. RB was treated thermally and chemically to increase its adsorption capacity. For thermal treatment (TTB), the bentonite was heated at 400 °C for 60 min, and for the chemical modification, its surface was treated by cetyltrimethylammonium bromide (CTAB) to prepare organo-modified bentonite (CTAB-B). The removal of Congo red dye (CR) from aqueous solution was investigated in the batch mode. The prepared adsorbents were characterized by SEM, BET, and FTIR analyses. The effects of various experimental parameters such as contact time, pH, adsorbent dosage, dye concentration and temperature were investigated. The obtained results were in good agreement with the Langmuir isotherm model, and the maximum adsorption capacity of RB, TTB and CTAB-B was 43.1, 55.86 and 116.28 mg/g, respectively. The adsorption kinetic was better described by the pseudo-second order kinetic model. The results showed that thermally or chemically modified bentonite could be proposed as a low-cost adsorbent for the removal of CR from water.

1. Introduction

The application of dyes in many industries such as textile, printing and dyeing may cause the discharge of large amounts of colored wastewater that results in environmental pollution [1]. Most of the dyes are chemically stable and carcinogenic materials which are thermally and chemically resistant besides being complex aromatic structures [2,3]. Nowadays, the treatment of wastewaters containing these compounds is carried out to protect public health and the environment. Such contamination is of a global concern. Congo red is an anionic dye applied as a pH indicator, and it may also be used as histological stain for amyloid. CR is a toxic dye and even low concentrations can affect humans. So utilizing an applicable process for its removal from industrial wastewaters is important [3]. everal methods have been used for the removal of dyes from aqueous solutions: membrane filtration [4] coagulation [5], ozonation [6], chemical or photochemical oxidation or degradation [7], etc. Among these methods, adsorption is recognized as a conventional and cost efficient method which includes no additional sophisticated treatment steps. Furthermore, this method has many other advantages including high efficiency, easy handling, simplicity in operation, and produces no harmful by-products [8,9]. Up until now, various materials have been proposed as adsorbents for decolorization. Activated carbon is one of the best examined materials with a suitable capacity of adsorption, but it is relatively expensive and its regeneration is difficult. Reasonably, researchers have focused on low cost adsorbents to reduce process costs [10]. The use of low-cost adsorbents such as clay for dye removal has been considered in recent years. These minerals have many advantages such as low cost, availability, high adsorption capacity, non-toxicity, chemical and mechanical stability, layered structure, large specific surface area, and easy regeneration [11]. Bentonite is defined as a common clay that is constructed from two tetrahedral silica sheets with an octahedral alumina layer. This mineral has excellent characteristics such as high

*Corresponding author. Tel.: +982177240496
E-mail address: norouzbeigi@iust.ac.ir
DOI: 10.22104/AET.2018.1844.1088

specific surface area, high ion exchange capacity, porous structure and high adsorption capacity. The negative charge of the bentonite surface results from the isomorphic substitution of Al^{3+} for Si^{4+} in the tetrahedral sheet and Mg^{2+} for Al^{3+} in the octahedral one. Thereafter, the anionic charge of the alumina-silicate layer is neutralized by the interaction of exchangeable cations (e.g. Na^+, Ca^{2+} and/or Mg^{2+}) [12]. Bentonite has been used widely as an adsorbent for removing cationic compounds using a combination of adsorption and ion exchange processes. However, anionic dyes and compounds can only be adsorbed onto the external surface of bentonite in negligible amounts [13]. Therefore, some surface modifications should be carried out in order to improve its adsorption capacity. One of the reliable methods examined is acid activation. In acid activation, the sorbent porosity increases based on structural changes [14]. Besides the physico-chemical properties of the bentonite, it can be modified by applying other methods such as thermal treatment. This kind of treatment leads to the delamination of the aluminosilicate layers [15]. The acid activation route followed by thermal treatment can successfully increase the adsorption capacity [16]. Alternatively, the organic modification process can be introduced as another suitable route. In this way, the hydrophilicity of the mineral can be decreased, and the sorbent surface wettability may be changed from a hydrophilic to a hydrophobic (organophilic) state by the interaction of inorganic exchangeable cations (Na^+, K^+, Al^{3+} and Ca^{2+}) with long chain cationic surfactants. The obtained complex is called organoclay [17,18]. Such organophilic bentonite can be applied as a catalyst [19] and adsorbent for the removal of organic pollutants from the aqueous solution [20,21]. The chemical modification method has been used for the removal of reactive blue 19 by using 1,6-diamino hexane modified bentonite [22] and weak acid scarlet by chitosan modified bentonite [23]. Thermal and chemical modifications of bentonite have been studied for the first time in order to increase the removal of Congo red (an anionic dye). First, raw bentonite was thermally modified and then treated chemically by CTAB as a cationic surfactant that resulted in (CTAB-B). The prepared adsorbents were characterized and their adsorption capacities were evaluated. The results showed that the adsorption capacity of bentonite could be successfully improved using chemical and thermal modifications.

2. Materials and methods

2.1. Materials

Raw bentonite was obtained from the Kanisaz Jam Company (Iran). In the first step, 100 g of bentonite was washed and dispersed in water several times to remove the impurities. The obtained suspension was filtered through filter paper. The solid sample was dried at 90 °C for 24 h. Congo red and cetyltrimethyl ammunium bromide (surfactant) were supplied by the Merck Company (Germany). The molecular structures of the dye and surfactant are shown in Figures 1 and 2, respectively. The molecular weight of CR was 696.66 g/mol. This chemical was used without further purification. For preparing the solutions, the desired amounts of dye were dissolved in deionized water.

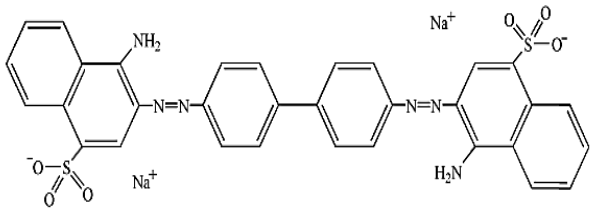

Fig. 1. Molecular structure of Congo red

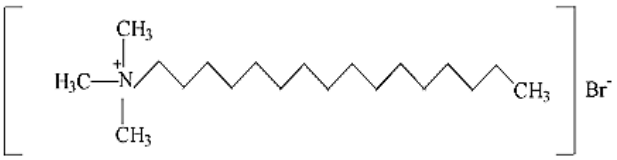

Fig. 2. Molecular structure of cetylerimethyammunium bromide

2.2. Adsorbents Modification

To prepare the CTAB-B Sorbent, 20 g of RB was added to a 200 ml solution containing CTAB (0.4 M), and the mixture was stirred for 24 h at room temperature. The mixture was filtered, and the powders were washed with the deionized water several times. The CTAB-B was dried in an oven (50 °C) for 24 h and screened through a #100 mesh sieve. For the thermal treatment of the bentonite (TTB), specific amounts (5 g) of raw bentonite were heated at 400 °C in a muffle furnace for 1 h and the output was sieved (#100 mesh).

2.3. Characterization

The chemical composition of the used bentonite was determined using X-ray fluorescence spectroscopy (XRF) analysis (Philips, PW 1800). The morphology of the adsorbents were evaluated by scanning electron microscopy (SEM) using a VEGA TESCAN scanning electron microscope. The specific surface area, average pore size and pore volume were measured using the N_2 gas sorption method using a PHS-1020 (PHSCHINA) analyzer. The IR spectra of the samples were obtained using a FTIR Spectrophotometer (Perkin Elmer Spectrum, RX1, Germany) in order to determine the surface functional groups.

2.4. Adsorption experiments

In order to study the effect of different parameters such as contact time, solution pH, initial concentration and temperature on the adsorption of CR onto the RB, TTB and CTAB-B, the batch adsorption method was carried out in vessels (250 ml) containing 100 ml of the solution

(100 mg/L). The mixtures were shaken in a rotary incubator at 120 rpm until adsorption equilibrium was achieved, then the adsorbent was removed and centrifuged at 6000 rpm (Hettich EBA 20). The concentrations of dye solutions were measured using a UV-Vis spectrometer (T80 UV/VIS spectrometer, PG Instrument Ltd.) at the wavelength corresponding to the maximum absorbance at 500 nm. The pH values were adjusted by diluted solutions (0.5 molar) of HCl and NaOH. The adsorption capacity, q_e (mg/g), was calculated by Equation 1:

$$q_e = \frac{C_0 - C_e}{M} \times V \quad (1)$$

where C_e (mg/L) is the liquid phase concentration of dye at the equilibrium state, V is the volume of the solution (L), and M is the consumed amounts of the adsorbent (g) which is considered as the adsorbent dosage.

3. Results and discussion

3.1. Adsorbent characterization

Table 1 shows the results of the elemental analysis of the used RB. From the results, it can be concluded that silica and alumina are the major constituents along with traces of iron, magnesium, calcium, sodium, potassium, and titanium oxides. The SEM micrographs of RB, TTB and CTAB-B are shown in Figure 3. The surface morphology of the bentonite has changed slightly by thermal modification (Figure 3b). Due to the evaporation and elimination of water from the bentonite at high temperatures, it has formed a rougher surface [15]. According to Figure 3c, it can be seen that the CTAB molecules can slightly fill the smaller pores and may result in a smoother surface. Similar results have been reported [24].

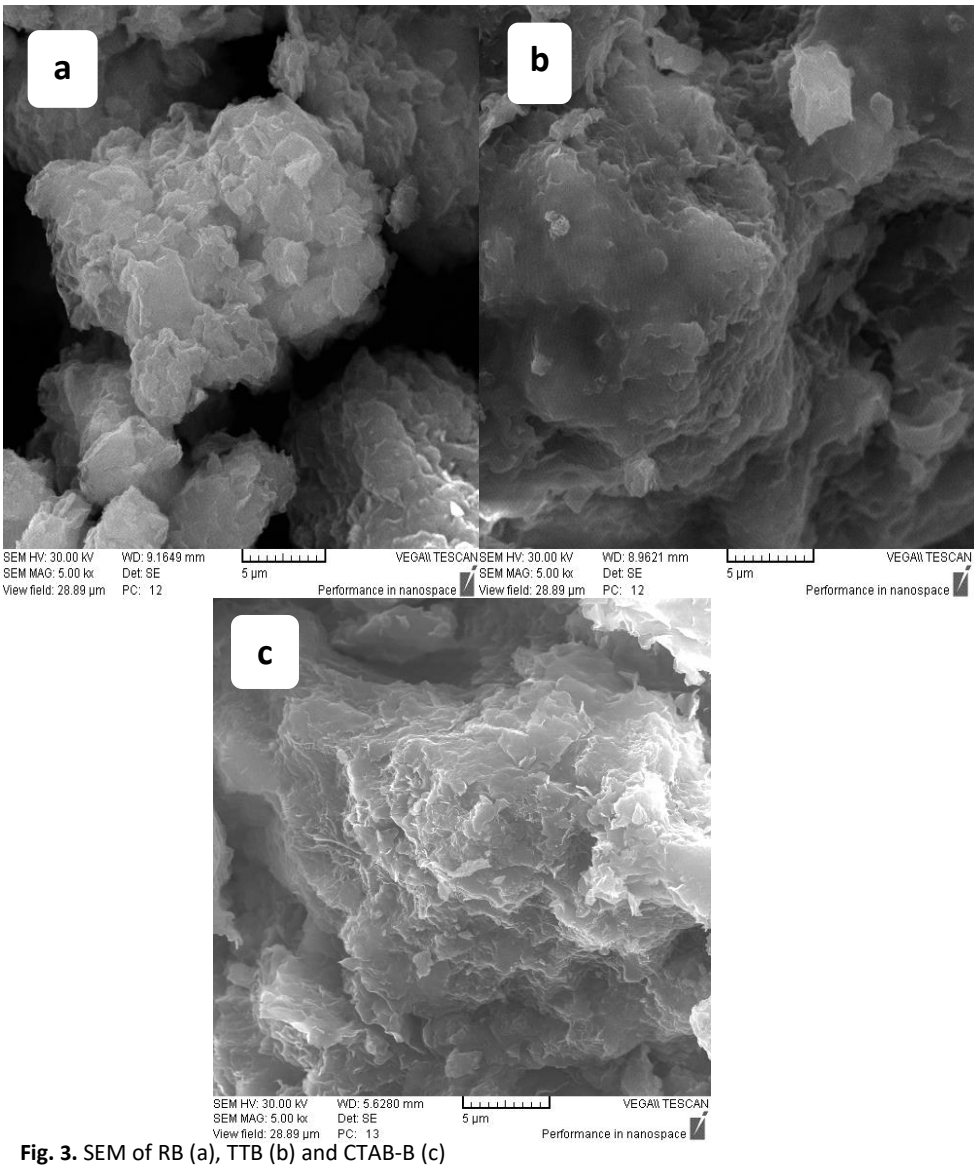

Fig. 3. SEM of RB (a), TTB (b) and CTAB-B (c)

Table 1. The chemical composition of RB

compound	SiO_2	AL_2O_3	Fe_2O_3	MgO	CaO	Na_2O	K_2O	TiO_2	LOI[a]
Weight percent	69.965	16.311	1.342	3.55	1.742	0.245	1.002	0.192	5.653

[a] loss of ignition

The resulting textural data from the N_2 adsorption/desorption evaluation are listed in Table 2. According to the obtained data, the average Brunauer–Emmett–Teller (BET) surface area of CTAB-B decreased. It can be attributed to the occupation of the exchanging sites with CTAB, the inaccessibility of the internal surface, and as reported by other researches, the formation of large pores on the sorbent surface [13]. The lower pore volume of CTAB-B compared to that which was obtained for RB can be related to pore fillings by the macro molecules of CTAB. The increase of pore volume after thermal modification is a result of water loss and cavity expansions after water withdrawal. As it was mentioned, the thermal modification of bentonite can make it more porous, and the distance between the bentonite layers can be increased. It leads to an increase of the surface area, pore diameter and pore volume [25,26].

Table 2. Adsorbents textural data

adsorbent	RB	TTB	CTAB-B
surface area (m^2/g) BET	41.81	43.38	36.45
Average pore diameter (nm)	2.337	2.344	2.347
Pore volume (cm^3/g)	0.135	0.148	0.128

The FTIR spectra of RB, CTAB and CTAB-B are demonstrated in Figure 4. The results for RB and TTB are showed in Figure 5. The obtained graphs revealed that the existence of the functional groups on the surfaces of the adsorbents were qualitatively based on the characteristic absorbed energy for each bond of certain groups [13]. The broad bands observed at 3626 cm^{-1} referred to the O–H stretching vibrations of the silanol (Si–OH) groups [8]. The band presented at 3434 cm^{-1} corresponded to the –OH stretching vibration of H_2O. The peak that appeared at 1638 cm^{-1} may be due to H–O–H bending vibrations. The decrease of the peak intensity can be related to H_2O content reduction due to the exchange of the hydrated cations by the used surfactant ions [9]. The band that appeared at 1032 cm^{-1} showed the Si-O vibration. The stretch vibrations of Al-O-Si and Al-O groups were the references of the peaks that appeared at 774 cm^{-1} and 520 cm^{-1}, respectively [12]. As it is shown in the spectrum of the organo-bentonite sample, two peaks appeared at 2920 cm^{-1} and 2850 cm^{-1} that could be related respectively to the asymmetric and symmetric stretching vibrations of the $-CH_3$ and $-CH_2$ groups of the aliphatic chain of the surfactant. The peak observed at 1480 cm^{-1} may refer to the shearing vibration. This observation indicated that an interaction reaction occurred during the modification process of the bentonite by CTAB [18]. From the FTIR spectrum of TTB, it can be inferred that the bands related to the water molecules changed after thermal modification. The intensities of the peaks at 3434, 1638 and 3626 cm^{-1} decreased. The results showed water withdrawal and loss of the hydroxyl groups. Similar results have been reported for calcination of bentonite at 500 °C by Vieira et al. [25].

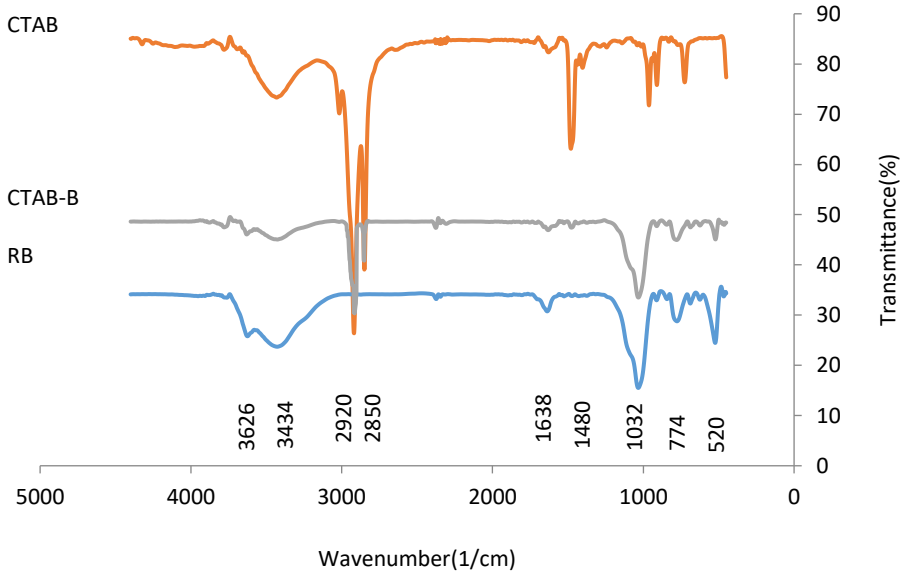

Fig. 4. FTIR of RB, CTAB and CTAB-B

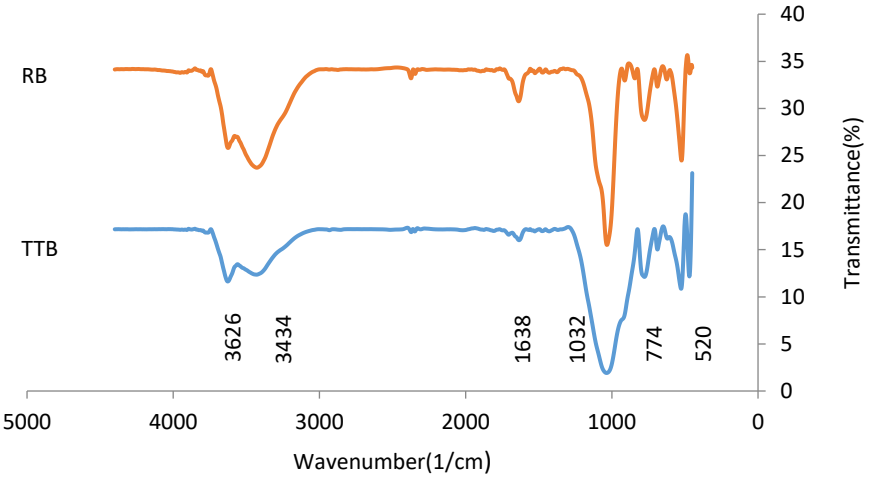

Fig. 5. FTIR of RB and TTB

3.2. Effect of contact time

The effect of contact time on the adsorption of CR by RB, TTB and CTAB-B is shown in Figure 6. In order to determine the equilibrium time, batch experiments were carried out with 100 ml of CR solution with a fixed adsorbent dosage (0.2 g). The solution temperature and pH were fixed at 23 °C and 7, respectively. Three different dye concentrations (20, 100 and 250 mg/L) were tested. During the first 30 min, the amounts of the adsorbed dye onto the adsorbent increased rapidly because of the availability of the adsorbing sites in the first steps. Therefore, the dye molecules were easily adsorbed on the existing sites [8]. Then, as time passed, the adsorption process did not continue so fast, and the rates of adsorption gradually trended to the zero value; this was due to repulsive forces that existed between the CR molecules adsorbed on the adsorbents and those present in the solution [3]. So after about 180 min, a dynamic equilibrium state was achieved. At this time, the amount of CR adsorbed on the RB, TTB and CTAB-B per unit amount of adsorbent was 12.05, 32.92 and 47.14 mg/g, respectively. Accordingly, 180 min was selected as the contact time for further experiments.

3.3. Kinetics studies

Several adsorption kinetic models have been derived to evaluate the diffusion mechanism involved during the adsorption process. In this study, the kinetics of CR adsorption onto RB, TTB and CTAB-B was studied in terms of pseudo-first-order and pseudo-second-order kinetic models besides the intraparticle diffusion model. The pseudo-first order or Lagergren's kinetics equation explains liquid–solid phase adsorption systems and describes the adsorption rate based on the adsorption capacity. The linear form of the pseudo-first order kinetics model is expressed as follows (Eq. 2) [27]:

$$\log(q_e - q_t) = \log q_e - \frac{k_1}{2.303} t \quad (2)$$

where q_e and q_t are the amounts of solute adsorbed at the moments of equilibrium (mg/L) and t (min), respectively. k_1 (min^{-1}) is the rate constant for the pseudo-first-order reaction. From the slope and intercept of the log(q_e-q_t) versus t linear plot, the constant k_1 and equilibrium adsorption capacity (q_e) can be calculated. Table 3 indicates that the differences between the calculated (predicted) values and the experimental data are significant. Accordingly, the second model was evaluated.

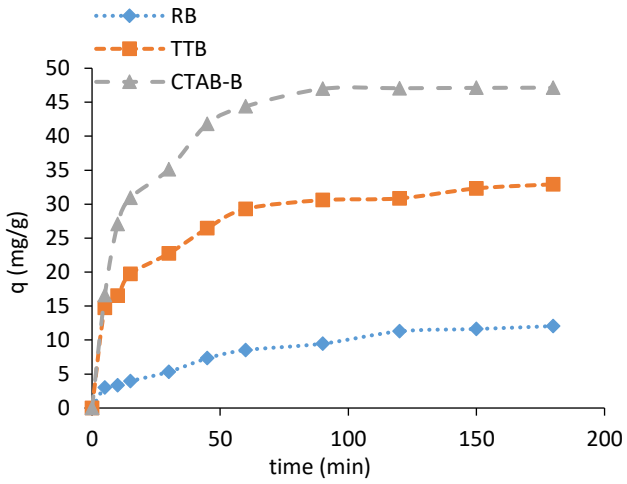

Fig. 6. Effect of contact time on the adsorption of CR on RB, TTB and CTAB-B

Table 3. The pseudo-first order kinetic model constants for the adsorption of CR on the RB, TTB and CTAB-B

adsorbent	Initial concentration (mg/L)	$q_{e\ exp}$ (mg/g)	q_e cal (mg/g)	K_1 (min^{-1})	R^2
RB	100	12.05	11.83	0.020	0.9639
TTB	20	8.85	7.56	0.019	0.8874
TTB	100	32.92	17.61	0.019	0.9357
TTB	250	58.18	34.74	0.039	0.8148
CTAB-B	20	9.80	12.14	0.691	0.9905
CTAB-B	100	47.14	38.18	0.048	0.9892
CTAB-B	250	100.42	71.00	0.046	0.9639

A pseudo-second order kinetic model [27] in the linear form is given by Eq. 3:

$$\frac{t}{q_t} = \frac{1}{k_2 q_e^2} + \frac{t}{q_e} \quad (3)$$

where k_2 (g min^{-1}) is the rate constant of the pseudo-second-order model. This model is usually used to describe chemisorption as well as cation exchange reactions [27]. The constant of the model and q_e can be obtained from the slope and intercept of the t/q_t versus t plot. The pseudo-second order constant, the computed q_e values and corresponding linear regression correlation coefficient values (R^2) are given in Table 4. As it can be seen in Table 4, the calculated values agree well with the experimental data. The linear correlation coefficients related to all cases are almost near to unity. The results show that the adsorption of CR onto RB, TTB and CTAB-B follow the pseudo-second-order model better than the other. The pseudo-second-order rate constant (k_2) decreases when the CR concentration increases because of the existence of high competition for access to the adsorbent active sites in higher concentrations [2]. Similar results have been reported for the adsorption of CR onto Mg–Fe–Cl layered double hydroxides and vaterite calcium [28,2].

Table 4. The pseudo-second order kinetic model constants for the adsorption of CR on the RB, TTB and CTAB-B

adsorbent	Initial concentration (mg/L)	$q_{e\ exp}$ (mg/g)	$q_{e\ cal}$ (mg/g)	K_2*10^3 (g/mg.min^{-1})	R^2
RB	100	12.05	14.83	1.71	0.9873
TTB	20	8.85	9.46	4.85	0.9956
TTB	100	32.92	34.48	2.56	0.9977
TTB	250	58.18	61.35	1.96	0.9989
CTAB-B	20	9.80	9.80	684.00	0.9997
CTAB-B	100	47.14	50.00	2.19	0.9900
CTAB-B	250	100.42	105.2	1.22	0.9989

The intra-particle diffusion model is used for identifying the adsorption mechanism in process design purposes. The linear form of the model can be introduced by the Eq. 4 [29]:

$$q_t = C + k_i t^{\frac{1}{2}} \quad (3)$$

where k_i is the intraparticle diffusion rate constant (mg g^{-1} $min^{-1/2}$). The value of k_i can be obtained by plotting q_t against $t^{1/2}$. C is indicative of the boundary layer thickness. Higher amounts of C mean higher boundary layer thickness. Whenever intraparticle diffusion occurs, q_t values versus $t^{1/2}$ will be fitted well by a linear equation. If the obtained plot passes through the origin, the intraparticle diffusion will be the only rate limiting process. Otherwise, some other mechanisms along with the intraparticle diffusion may also be involved [29,30]. The results showed that the experimental data could be separated to three distinct linear regions. This meant that there were three distinct adsorption stages. The first region was related to the external surface adsorption when the adsorbate diffused through the solution to the external surface of the adsorbent. This stage was completed in a short time

because the initial concentration of the solute was high, and the large concentration gradient provided a sufficient and suitable driving force for CR diffusion to the external surface of the adsorbent. The second region can be reasonably related to the intra-particle diffusion stage. The third one was the final equilibrium stage in which the intraparticle diffusion started to slow down due to the extremely low concentrations of the adsorbate left in the solution [31]. The intraparticle diffusion constants (k_i) and the linear correlation coefficients (R^2) are listed in Table 5. Observing the data, it can be inferred that the second step can be introduced as the main resistance (limiting step) of the mass transfer operation. Similar results have been reported for the adsorption of CR onto sodium bentonite, kaolin, zeolite [11] and CS-m-GMCNT composites [32].

Table 5. Intraparticle diffusion model constants for adsorption of CR on the CTAB-B

parameters	RB	TTB	CTAB-B
k_{i1}(mg.g.min$^{-0.5}$)	0.57	3.00	8.86
k_{i2}(mg.g.min$^{-0.5}$)	1.02	2.89	4.11
k_{i3}(mg.g.min$^{-0.5}$)	0.63	0.64	0.004
C_1 (mg/g^1)	1.68	7.73	-2.50
C_2(mg/g)	0.18	6.96	13.11
C_3(mg/g)	3.85	24.29	46.57
R_1^2	0.9471	0.9463	0.9667
R_2^2	0.9355	0.9993	0.9606
R_3^2	0.9913	0.9232	0.9772

3.4. Effect of pH

The initial pH of the solution can affect the structure of the CR molecules. This dye exhibits different colors at difference pH values (the color of CR changes from dark blue to red when the pH value shifts from 3 to 5) [33]. So, for investigation of the solution pH effect, several experiments were conducted in the pH ranges from 3 to 10. Figure 7 illustrates the obtained data for the batch experiments. In each experiment, 0.2 g of adsorbent was added into 100 ml of dye solution with an initial CR concentration of 100 mg/L at 23 °C. Different initial pH values were tested. The results showed that the amounts of dye adsorbed did not change significantly in the pH range of 3 to 10. The final amount of the solution pH was ~ 7. This implied that the retention of H^+ or OH^- of clay fractions made the solution neutral [34]. Similarly, it has also been observed for the adsorption of phenol onto CTAB-B in acidic solutions [8].

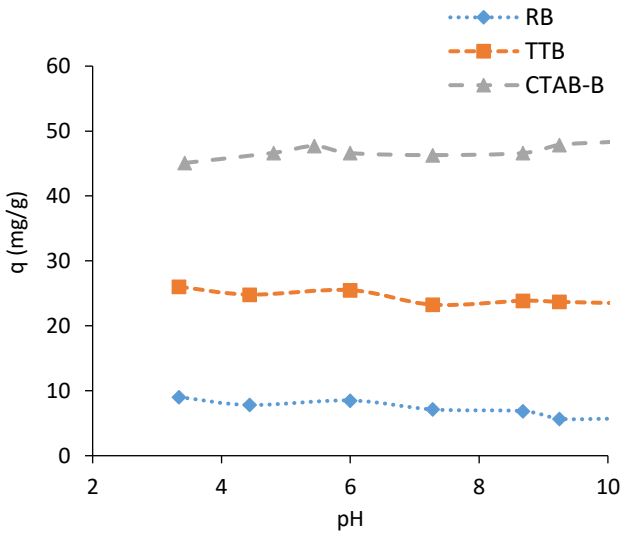

Fig. 7. Effect of solution pH on the adsorption of CR on RB, TTB and CTAB-B

3.5. Effect of adsorbent dosage

The effect of the adsorbent dosage on the dye removal efficiency and the adsorption uptake was studied (Figure 8). To investigate this parameter, batch experiments were conducted using 100 mL of dye solutions with fixed initial concentration (100 mg/L). Accordingly, different amounts of adsorbent dosage (0.05-1 g) were tested. It was observed that the uptake of dye increased rapidly with increasing of the adsorbent from 0.05 g to 0.2 g, and it remained constant for further increase of the adsorbent dosage. The dosage of 0.2 g was chosen as the optimized value for further experiments. When the amount of the adsorbent increased from 0.05 g to 0.2 g, the adsorption sites and accordingly the removal efficiency increased [27,35]. After this point, increasing the adsorbent caused aggregation of the particles and consequently, the adsorbent site decreased [8].

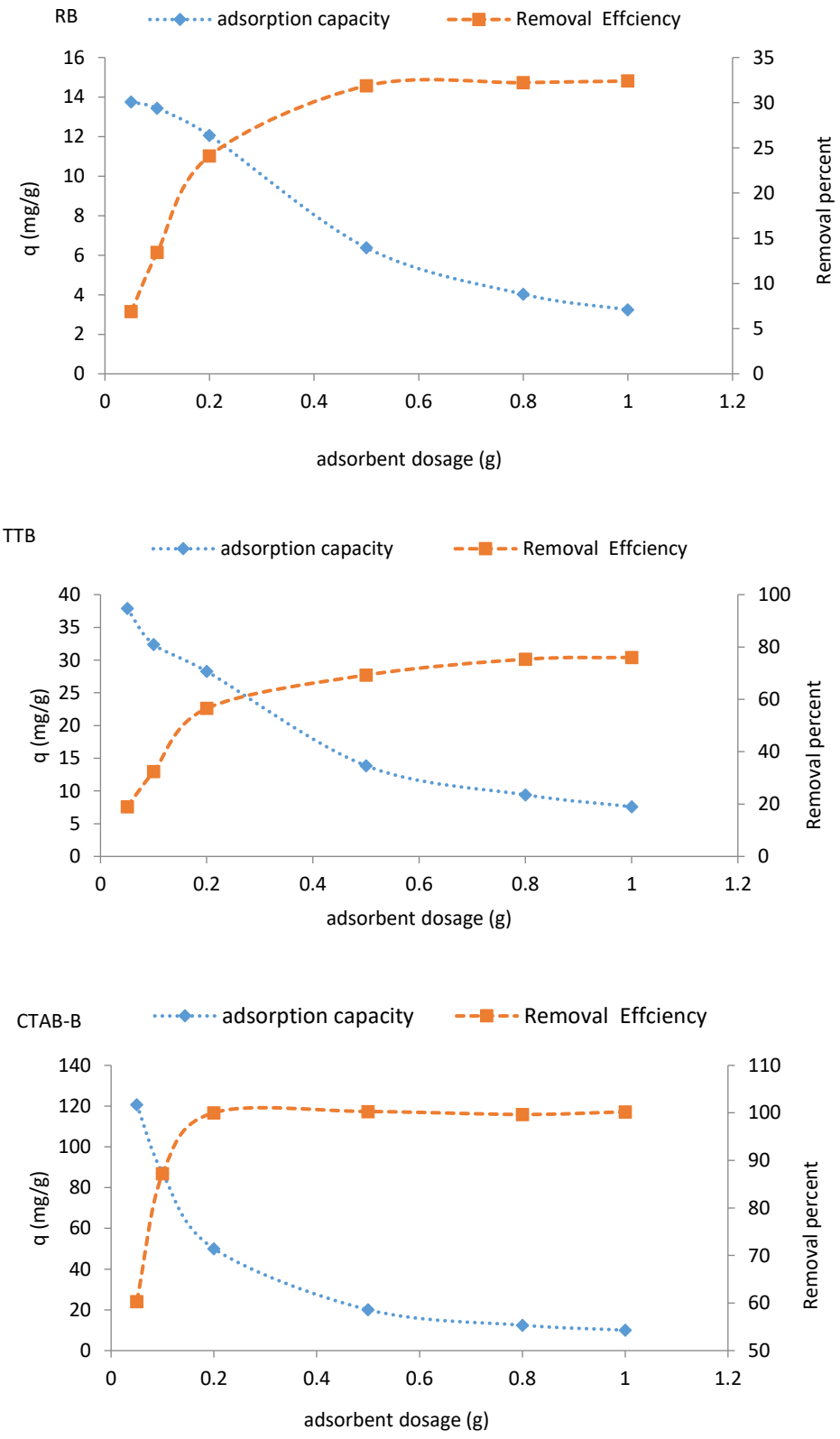

Fig. 8. Effect of adsorbent dosage on the adsorption of CR onto RB, TTB and CTAB-B

3.6. Initial dye concentration

The effect of initial dye concentration was investigated in the range of 20 to 250 mg/L. The obtained data showed that when the initial adsorbate concentration increased from 20 to 250 mg/L, the amounts of q_e increased. The diffusion of the molecules depended on the initial solute concentration, so increasing the initial adsorbate concentration increased the driving force of the mass transfer [33]. As a result, the adsorption capacities related to higher initial CR concentrations were greater than the others. The results are illustrated in Figure 9.

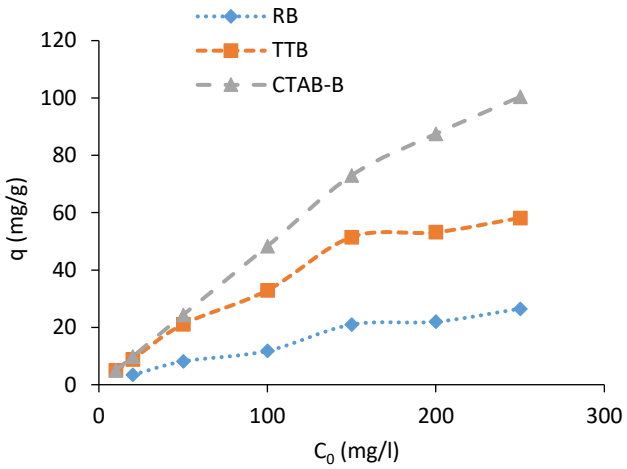

Fig. 9. Effect of adsorbate dosage on the adsorption of CR onto RB, TTB and CTAB-B

3.7. Adsorption isotherm models

In order to describe the interaction and equilibrium relationship between the adsorbent surface and the adsorbate molecules, the isotherm models can be investigated [33]. In this study, the Langmuir and Freundlich isotherms were applied to explain the dye-clay interactions. The Langmuir isotherm assumption is based on the presence of uniform and homogenous adsorption sites. Also, it is assumed that there is no interaction between the adsorbed molecules and the surface atoms [35]. Thus, a monolayer of adsorbates will build up, and the adsorption energies related to all of the sorbing sites will be the same [36,37]. The non-linear and linear forms of the Langmuir isotherm are as follows (Eq. 5 and 6) [8]:

$$q_e = \frac{q_m k_L C_e}{1 + k_L C_e} \quad (5)$$

$$\frac{1}{q_e} = \frac{1}{q_{max}} + \frac{1}{k_L q_{max} C_e} \quad (6)$$

In the equations, C_e is the equilibrium concentration of the solute (mg/L), q_{max} (mg/L) is the maximum monolayer adsorption capacity, and k_L (L/mg) is the Langmuir constant which relates to the energy or net enthalpy of adsorption [8]. This parameter represents the chemical affinity between the absorbent and adsorbed dye molecules. q_{max} and k_L can be calculated from the slope and intercept of the linear plot of $1/q_e$ versus $1/C_e$, respectively. The Freundlich isotherm deals with non-ideal, reversible and multilayer adsorption onto heterogeneous surface energy systems. The assumption of the model is that the amounts of the energy relating to the sorption sites are not the same. So the sites having higher energy levels will be filled first [33]. The Freundlich isotherm model can be expressed by Eq. 8 [3]:

$$q_e = k_f C_e^{1/n} \quad (8)$$

The linear form is presented by Eq. 9:

$$\ln q_e = \ln k_f + \frac{1}{n} \ln C_e \quad (9)$$

where k_f and n are Freundlich adsorption isotherm constants, being indicative of the extent of the adsorption and the degree of nonlinearity between solution concentration and adsorption, respectively [34]. The parameters can be easily determined from the linear plot of $\ln q_e$ versus $\ln C_e$. The obtained values from the linear equation are listed in Table 6. The amounts of n constant are higher than 1. It means that the dye removal process can be assumed as a favorable chemisorption under the examination conditions [3]. As it is shown in Table 6, the Langmuir isotherm fits well with the experimental data (R^2>0.99) in comparison with the Freundlich isotherm (R^2=0.8498-0.9775). So there is a monolayer coverage of dye and homogeneous distribution of active sites [33,34]. Similar results have been obtained in the adsorption of CR onto types of kaolin by Vimonses et al. [35]. The essential features of the Langmuir isotherm can be expressed in terms of a dimensionless constant called the separation factor (R_L, also called equilibrium parameter), which is defined as Eq. 10.

$$R_L = \frac{1}{1 + bC_0} \quad (10)$$

where C_0 (mg/L) is the initial CR concentration and b (L/mg) is the Langmuir constant related to the energy of adsorption. R_L values indicate the shape of the isotherm to be either unfavorable (R_L > 1), linear (R_L = 1), favorable (0 < R_L <1) or irreversible (R_L = 0) [38]. The calculated values are given in Table 6. The R_L values which are less than 1 and greater than 0 indicate favorable adsorption.

The adsorption capacities of some other adsorbents used for CR removal are presented in Table 7. Evaluation of the data indicates that TTB and CTAB-B have suitable and desirable adsorption capacities. The simplicity of the introduced modification method, besides the low-cost and availability of the adsorbents, can be considered as the relative advantage of this study for CR removal.

Table 6. The isotherm constants of the adsorption of CR onto RB, TTB and CTAB-B

	parameter	RB	TTB	CTAB-B
Langmuir	q_m (mg/g)	43.10	55.86	116.28
	k_L (L/mg)	0.006	0.081	0.229
	R_L	0.93-0.37	0.50-0.04	0.30-0.02
	R^2	0.9928	0.9917	0.9960
Freundlich	k_F ($mg^{1-1/n}.L^{1/n}.g^{-1}$)	0.53	6.97	22.20
	n (g/L)	1.336	2.178	2.180
	R^2	0.9775	0.9538	0.8498

The adsorption capacities of some other adsorbents used for CR removal are presented in Table 7. Evaluation of the data indicates that TTB and CTAB-B have suitable and desirable adsorption capacities. The simplicity of the introduced modification method, besides the low-cost and availability of the adsorbents, can be considered as the relative advantage of this study for CR removal.

Table 7. Previously reported adsorption capacities of various adsorbents for CR

Adsorbent	Capacity (mg/g)	reference
Red mud	4.05	[11]
Q38 Kaolin	5.44	[35]
K15GR Kaolin	6.81	[35]
Ceram Kaolin	7.27	[35]
Vaterite $CaCO_3$	16.53	[2]
Fe_3O_4 graphene composite (FGC)	33.66	[39]
RB	43.10	This study
perlite	55.55	[38]
TTB	55.86	This study
ZrO_2 hollow spheres	59.5	[31]
HDTMA-vermiculite organovermiculite	76.92	[40]
$Ni(OH)_2$ Nano sheets	82.9	[41]
Mg–Fe–Cl Layered double hydroxides	104.6	[28]
CTAB-B	116.28	This study
NiO/graphene nanosheets (NGNS)	123.89	[27]
magnetic $Ni_{0.5}Zn_{0.5}Fe_2O_4$ nanoparticles	204.82	[29]

4. Conclusions

The dye adsorption capacity of the bentonite was improved successfully via thermal modification. In order to create an organo-clay adsorbent, chemical modification of the bentonite was carried out by a CTAB cationic surfactant. The batch adsorption experiments showed that the amount of dye adsorption capacity increased with increasing of the initial dye concentration, but little change occurred with the increase of the solution pH. It was also observed that 0.2 g of CTAB-B could remove 99% of CR with an initial concentration of 100 mg/L. The kinetics and isotherms were studied, and the experimental results were best described by the pseudo-second-order kinetic model and Langmuir isotherm, respectively. The maximum monolayer adsorption capacity of CTAB-B was found to be 116.28 mg/g. The obtained results showed that thermal and chemical modification of the bentonite could successfully increase the CR adsorption capacity.

Acknowledgments

The authors gratefully acknowledge the research council of the Iran University of Science and Technology.

References

[1] Sharma, P., Kaur, H., Sharma, M., Sahore, V. (2011). A review on applicability of naturally available adsorbents for the removal of hazardous dyes from aqueous waste. *Environmental monitoring and assessment*, *183*(1-4), 151-195.

[2] Chong, K.Y., Chia, C.H., Zakaria, S., Sajab, M.S. (2014). Vaterite calcium carbonate for the adsorption of Congo red from aqueous solutions. *Journal of environmental chemical engineering*, *2*, 2156–2161.

[3] Srilakshmi, C., Saraf, R. (2016). Ag-doped ydroxyapatite as efficient adsorbent for removal of Congo red dye from aqueous solution: Synthesis, kinetic and equilibrium adsorption isotherm analysis. *Microporous and mesoporous materials*, *219*, 134-144.

[4] Ghaemi, N., Madaeni, S. S., Daraei, P., Rajabi, H., Shojaeimehr, T., Rahimpour, F., Shirvani, B. (2015). PES

mixed matrix nanofiltration membrane embedded with polymer wrapped MWCNT: Fabrication and performance optimization in dye removal by RSM. *Journal of hazardous materials*, *298*, 111-121.

[5] Wei, Y., Ding, A., Dong, L., Tang, Y., Yu, F., Dong, X. (2015). Characterisation and coagulation performance of an inorganic coagulant—poly-magnesium-silicate-chloride in treatment of simulated dyeing wastewater. *Colloids and surfaces A: Physicochemical and engineering aspects*, *470*, 137-141.

[6] Basiri Parsa, J., Hagh Negahdar, S. (2012). Treatment of wastewater containing Acid Blue 92 dye by advanced ozone-based oxidation methods. *Separation and purification technology*, *98*, 315–320.

[7] Ucoski, G. M., Machado, G. S., de Freitas Silva, G., Nunes, F. S., Wypych, F., Nakagaki, S. (2015). Heterogeneous oxidation of the dye Brilliant Green with H_2O_2 catalyzed by supported manganese porphyrins. *Journal of molecular catalysis A: Chemical*, *408*, 123-131.

[8] Senturk, H. B., Ozdes, D., Gundogdu, A., Duran, C., Soylak, M. (2009). Removal of phenol from aqueous solutions by adsorption onto organomodified Tirebolu bentonite: Equilibrium, kinetic and thermodynamic study. *Journal of hazardous materials*, *172*(1), 353-362.

[9] Wang, L., Wang, A. (2008). Adsorption properties of Congo Red from aqueous solution onto surfactant-modified montmorillonite. *Journal of hazardous materials*, *160*(1), 173-180.

[10] Saikia, J., Das, G. (2014). Framboidal vaterite for selective adsorption of anionic dyes. *Journal of environmental chemical engineering*, *2*(2), 1165-1173.

11] Vimonses, V., Lei, S., Jin, B., Chow, C. W., Saint, C. (2009). Adsorption of congo red by three Australian kaolins. *Applied clay science*, *43*(3-4), 465-472.

[12] Zohra, B., Aicha, K., Fatima, S., Nourredine, B., & Zoubir, D. (2008). Adsorption of Direct Red 2 on bentonite modified by cetyltrimethylammonium bromide. *Chemical engineering journal*, *136*(2-3), 295-305.

[13] Koswojo, R., Utomo, R. P., Ju, Y. H., Ayucitra, A., Soetaredjo, F. E., Sunarso, J., Ismadji, S. (2010). Acid Green 25 removal from wastewater by organo-bentonite from Pacitan. *Applied clay science*, *48*(1-2), 81-86.

[14] Koyuncu, H., Kul, A. R. (2014). An investigation of Cu (II) adsorption by native and activated bentonite: kinetic, equilibrium and thermodynamic study. *Journal of environmental chemical engineering*, *2*(3), 1722-1730.

[15] Zivica, V., Palou, M. T. (2015). Physico-chemical characterization of thermally treated bentonite. *Composites part B: Engineering*, *68*, 436-445

[16] Salem, S., Salem, A., Babaei, A. A. (2015). Preparation and characterization of nano porous bentonite for regeneration of semi-treated waste engine oil: Applied aspects for enhanced recovery. *Chemical engineering journal*, *260*, 368-376.

[17] Khenifi, A., Zohra, B., Kahina, B., Houari, H., Zoubir, D. (2009). Removal of 2, 4-DCP from wastewater by CTAB/bentonite using one-step and two-step methods: a comparative study. *Chemical engineering journal*, *146*(3), 345-354.

[18] Motawie, A. M., Madany, M. M., El-Dakrory, A. Z., Osman, H. M., Ismail, E. A., Badr, M. M., Abulyazied, D. E. (2014). Physico-chemical characteristics of nano-organo bentonite prepared using different organo-modifiers. *Egyptian journal of petroleum*, *23*(3), 331-338

[19] Sedaghat, M. E., Booshehri, M. R., Nazarifar, M. R., Farhadi, F. (2014). Surfactant modified bentonite (CTMAB-bentonite) as a solid heterogeneous catalyst for the rapid synthesis of 3, 4-dihydropyrano [c] chromene derivatives. *Applied clay science*, *95*, 55-59

[20] Al-asheh, S., Banat, F., Abu-aitah, L. (2003). Adsorption of phenol using different types of activated bentonites. *Separation and purification technology*, *33*, 1–10.

[21] Nones, J., Nones, J., Riella, H. G., Poli, A., Trentin, A. G., Kuhnen, N. C. (2015). Thermal treatment of bentonite reduces aflatoxin b1 adsorption and affects stem cell death. *Materials science and engineering: C*, *55*, 530-537

[22] Gök, Ö., Özcan, A. S., Özcan, A. (2010). Adsorption behavior of a textile dye of Reactive Blue 19 from aqueous solutions onto modified bentonite. *Applied surface science*, *256*(17), 5439-5443.

[23] Guo, J., Chen, S., Liu, L., Li, B., Yang, P., Zhang, L., Feng, Y. (2012). Adsorption of dye from wastewater using chitosan–CTAB modified bentonites. *Journal of colloid and interface science*, *382*(1), 61-66.

[24] Kıranşan, M., Soltani, R. D. C., Hassani, A., Karaca, S., Khataee, A. (2014). Preparation of cetyltrimethylammonium bromide modified montmorillonite nanomaterial for adsorption of a textile dye. *Journal of the Taiwan Institute of chemical engineers*, *45*(5), 2565-2577.

[25] Vieira, M. G. A., Neto, A. A., Gimenes, M. L., Da Silva, M. G. C. (2010). Removal of nickel on Bofe bentonite calcined clay in porous bed. *Journal of hazardous materials*, *176*(1-3), 109-118.

[26] Zaghouane-Boudiaf, H., Boutahala, M., Sahnoun, S., Tiar, C., Gomri, F. (2014). Adsorption characteristics, isotherm, kinetics, and diffusion of modified natural bentonite for removing the 2, 4, 5-trichlorophenol. *Applied clay science*, *90*, 81-87.

[27] Rong, X., Qiu, F., Qin, J., Zhao, H., Yan, J., Yang, D. (2015). A facile hydrothermal synthesis, adsorption kinetics and isotherms to Congo Red azo-dye from aqueous solution of NiO/graphene nanosheets adsorbent. *Journal of industrial and engineering chemistry*, *26*, 354-363

[28] Ahmed, I.M., Gasser, M.S. (2012). Adsorption study of anionic reactive dye from aqueous solution to Mg–Fe–

CO_3 layered double hydroxide (LDH). *Applied surface science*, *259*, 650–656.

[29] Liu, R., Fu, H., Yin, H., Wang, P., Lu, L., Tao, Y. (2015). A facile sol combustion and calcination process for the preparation of magnetic $Ni_{0.5}Zn_{0.5}Fe_2O_4$ nanopowders and their adsorption behaviors of Congo red. *Powder technology*, *274*, 418-425.

[30] Shakir, K., Ghoneimy, H. F., Elkafrawy, A. F., Beheir, S. G., Refaat, M. (2008). Removal of catechol from aqueous solutions by adsorption onto organophilic-bentonite. *Journal of hazardous materials*, 150(3), 765-773.

[31] Wang, C., Le, Y., Cheng, B. (2014). Fabrication of porous ZrO_2 hollow sphere and its adsorption performance to Congo red in water. *Ceramics international*,40(7), 10847-10856

[32] Zhu, H., Fu, Y., Jiang, R., Yao, J., Liu, L., Chen, Y., Zeng, G. (2013). Preparation, characterization and adsorption properties of chitosan modified magnetic graphitized multi-walled carbon nanotubes for highly effective removal of a carcinogenic dye from aqueous solution. *Applied surface science*, *285*, 865-873

[33] Bulut, E., Ozacar, M., Sengil, I.A. (2008). Equilibrium and kinetic data and process design for adsorption of Congo Red onto bentonite. *Journal of hazardous materials*, *154*, 613–622.

[34] Lian, L., Guo, L., Wang, A. (2009). Use of $CaCl_2$ modified bentonite for removal of Congo red dye from aqueous solutions. *Desalination*, *249*(2), 797-801.

[35] Vimonses, V. u. a. (2009). Adsorption of congo red by three Australian kaolins. *Applied clay science*, *43*, 465–472

[36] Senturk, H. B., Ozdes, D., Gundogdu, A., Duran, C., Soylak, M. (2009). Removal of phenol from aqueous solutions by adsorption onto organomodified Tirebolu bentonite: Equilibrium, kinetic and thermodynamic study. *Journal of hazardous materials*, *172*(1), 353-362

[37] Tehrani-Bagha, A. R., Nikkar, H., Mahmoodi, N. M., Markazi, M., Menger, F. M. (2011). The sorption of cationic dyes onto kaolin: Kinetic, isotherm and thermodynamic studies. *Desalination*, *266*(1-3), 274-280.

[38] Vijayakumar, G., Dharmendirakumar, M., Renganathan, S., Sivanesan, S., Baskar, G., Elango, K. P. (2009). Removal of Congo red from aqueous solutions by perlite. *Clean–soil, air, water*, *37*(4-5), 355-364.

[39] Yao, Y., Miao, S., Liu, S., Ma, L. P., Sun, H., Wang, S. (2012). Synthesis, characterization, and adsorption properties of magnetic Fe_3O_4@ graphene nanocomposite. *Chemical engineering journal*, *184*, 326-332.

[40] Yu, X., Wei, C., Ke, L., Hu, Y., Xie, X., Wu, H. (2010). Development of organovermiculite-based adsorbent for removing anionic dye from aqueous solution. *Journal of hazardous materials*, *180*(1-3), 499-507.

[41] Cheng, B., Le, Y., Cai, W., Yu, J. (2011). Synthesis of hierarchical $Ni(OH)_2$ and NiO nanosheets and their adsorption kinetics and isotherms to Congo red in water. *Journal of hazardous materials*, *185*, 889–897